PHYSICAL REVIEW E **69**, 040901(R) (2004)

Diffuse scattering provides material parameters and electron density profiles of biomembranes

Yufeng Liu and John F. Nagle
Department of Physics, Carnegie Mellon University, Pittsburgh, Pennsylvania 15213, USA
(Received 3 September 2003; published 30 April 2004)

Fully hydrated stacks of DOPC lipid bilayer membranes generate large diffuse x-ray scattering that corrupts the Bragg peak intensities that are used in conventional biophysical structural analysis, but the diffuse scattering actually contains more information. Using an efficient algorithm for fitting extensive regions of diffuse data to classical smectic liquid crystalline theory we first obtain the compressional modulus $B=10^{13}$ erg/cm^4, which involves interactions between membranes, and the bending modulus $K_c=8\times10^{-13}$ erg of the membranes. The membrane form factor $F(q_z)$ is then obtained for most values of q_z up to 0.8 Å^{-1}. The electron density profile $\rho(z)$ is obtained by fitting models to $F(q_z)$. Constraining the models to conform to other measurements provides structural quantities such as area $A=72.1\pm0.5$ Å^2 per lipid at the interface.

DOI: 10.1103/PhysRevE.69.040901 PACS number(s): 87.14.Cc, 61.30.Cz, 87.16.Dg, 87.64.Bx

The ubiquity of membranes in biology and the important biochemical functions performed therein have motivated considerable study of their structure. Where do intrinsic and peripheral proteins reside with respect to the underlying lipid bilayer and how do the structural parameters of different lipid bilayers affect the functionality of these proteins? Structural studies are difficult, even for pure lipid bilayers, because these are soft condensed matter systems with many fluctuations that make the structure statistical rather than crystalline. Nevertheless, conventional structural biophysics has employed the approach of crystallographic x-ray diffraction on arrays of membranes. This works well with gel phase lipid bilayers [1]. However, the biologically relevant thermodynamic phase of lipid bilayers is the fluid L_α phase which, when fully hydrated, does not have enough higher orders of diffraction for crystallographic analysis. The reason for the disappearance of the higher orders of diffraction in well hydrated L_α phase systems follows from scattering theory of smectic liquid crystals [2,3] and is not due to a change in the structure of the membranes [4].

To observe more orders of diffraction the system may be partially dried, but then the quantitative bilayer structure changes. This change is quite drastic at 66% relative humidity [5,6]. It is less drastic when the relative humidity remains above 95%, but then the intensities of the higher diffraction orders must be corrected for fluctuations [4,6,7]. In either case the small amount of remaining water is thoroughly mixed with the headgroups of the lipid and there is little or no completely free aqueous space to compete for the more hydrophilic portions of added proteins [5,8].

The approach taken in our current work [9] differs from the conventional crystallographic approach by focussing on the diffuse intensity that is scattered throughout q space rather than on the integrated intensities in localized diffraction peaks. This approach has been employed for unoriented stacks of membranes [10,11]; unoriented stacks have the advantage, compared to the oriented stacks that are employed in this study, that the samples are easy to prepare with few artifacts. However, the intensity of the scattering decreases more rapidly with higher q_z due to the Lorentz factor; it is also not possible to extract both material moduli K_c and B independently, only the Caillé parameter $\eta = \pi k_B T/(2D^2\sqrt{BK_c})$ that contains their product [12]. Obtaining both K_c and B is possible using oriented samples as was shown by Lei *et al.* [13], but their method required high intensity of small angle scattering which only occurs for surfactant systems with values of bending moduli K_c that are much smaller than for biomembranes. We first showed that both moduli could be obtained by focussing on diffuse scattering in the range $q_z=0.2-0.6$ Å^{-1} and we reported values of the moduli for DOPC bilayers [9,14], as well as a preliminary form factor $F(q_z)$. We have subsequently improved our numerical analysis and taken more data under better conditions. We now report the electron density profile and the structural parameters describing the DOPC bilayer that we obtain from it.

Figure 1 shows a charge-coupled device (CCD) [15] image of the scattering observed from an oriented 10 μm thick film of DOPC lipid bilayers prepared using the rock and roll method on a flat Si substrate [16]. The flat sample was rotated continuously and uniformly with respect to the beam from $-1°$ to $8°$ ($q_z^{\max}=1.48$ Å^{-1} with wavelength 1.1808 Å) to ensure collection of data in the entire observable q_z range $0-0.8$ Å^{-1} with equal probability. Of course, the intensity recorded on a single CCD pixel comes from different values of q; this is taken into account in the analysis by integrating the theoretical intensity over the appropriate values of q.

The sample was placed in a specially designed humidity chamber. It has many of the same features as the Chalk River sample chamber [17] that was the first x-ray chamber to achieve full hydration [9]; this again demonstrates that the now defunct vapor pressure paradox was only an experimental artifact due to the difficulty of achieving 100 % relative humidity [18]. The primary data set in this paper has a repeat spacing $D=63.2$ Å, which is identical to that of unoriented dispersions in excess water [19].

Some of the data in the white box in Fig. 1 are shown quantitatively as a function of q_x in Fig. 2. $I(q_x)$ decays more rapidly when $q_z=2\pi h/D\approx0.1h$ Å^{-1} is near a lamellar order (integer values of h) than when q_z is between orders; as was previously emphasized [9], this is central to being able to obtain both K_c and B independently. Indeed, the fits to the data shown in Fig. 2 require the values of K_c and B that are given in Table I.

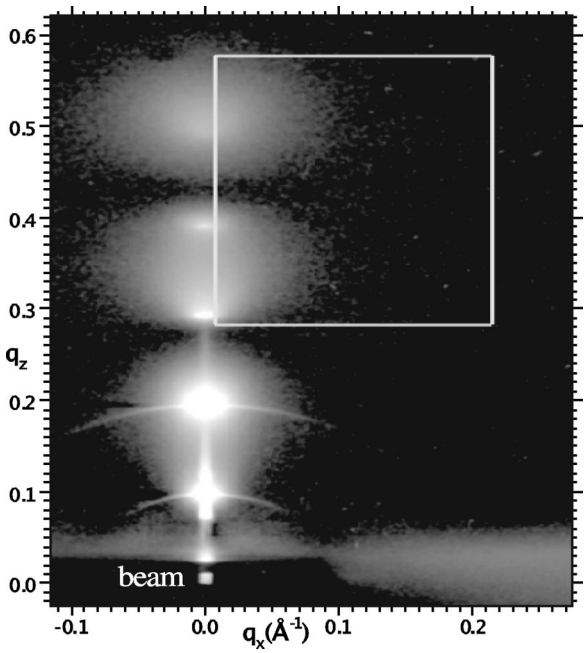

FIG. 1. Gray scale CCD image of fully hydrated DOPC bilayers with background scattering subtracted. The attenuated beam is visible at $q_z=0$. The white box shows the purely nonspecular scattering data that are analyzed to obtain the material parameters K_c and B; these data are uncontaminated by specular reflectivity visible along the meridian.

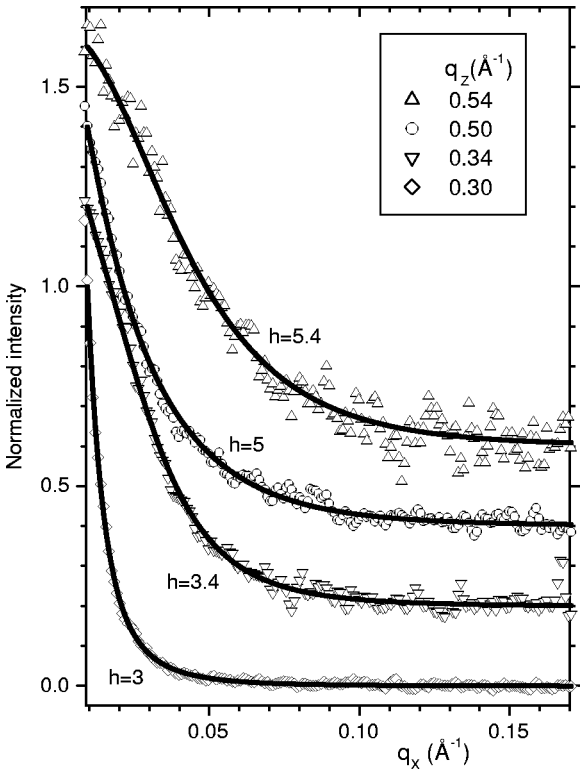

FIG. 2. Normalized scattering intensity I vs q_x are shown as data points for a few values of q_z with vertical offsets of 0.2 for successive q_z. The solid lines show the fits to the data that give the best values for the parameters shown in Table I and for the overall scaling factors that yield the bilayer form factors $|F(q_z)|$. The residuals to the fit (see Ref. [21]) are essentially random.

The theory behind the fits in Fig. 2 begins with the well-known smectic liquid crystal thermodynamic theory from which one obtains the height-height pair correlation functions that are used in the calculation of the scattering structure factor $S(q)$ [2] that is one of the factors in the intensity $I(q)=S(q)|F(q_z)|^2/q_z$ of the scattering shown in Fig. 1. Our calculation of $S(q)$ is similar to our previous presentation [9]. One change is in the cutoffs for the distance beyond which correlation functions are ignored. We had previously envisioned that such cutoffs would come from effective domain sizes, which would be the same in the two in-plane directions. The cutoffs could also come from the coherence lengths of the x-rays, so the calculation now allows for three cutoffs L_x, L_y, L_z, which are applied gradually with exponential distributions. As emphasized previously [9], the values of the cutoffs are of only secondary importance in fitting the data in the white box in Fig. 1. Once K_c and B were determined, fits to data dominated by the strong $h=1,2$ peaks at smaller q_z helped to determine the cutoff values $L_z=600$ Å and $L_x=L_y=15\,000$ Å [20] that we subsequently used. Other experimental features that were included in the calculation were geometric broadening due to the finite size of the x-ray beam, resolution broadening ($\delta q_z=0.0003$ Å^{-1} with a Ge double bounce monochromator and $\delta q_x=0.0001$ Å^{-1} with slits), and mosaic spread 0.1°. The nonlinear least squares program that fit K_c and B to the data required efficient code to calculate the theoretical correlation functions and then to implement these many experimental considerations in the calculation of $S(q)$ [21].

The theory fits the data very well as a function of q_x for 599 fixed values of q_z, as shown for just four q_z slices in Fig. 2. The primary parameters determined by the fit are the Caillé parameter η and the in-plane correlation length $\xi=(K_c/B)^{1/4}$, from which K_c and B are calculated with results shown in Table I for the fully hydrated sample with $D=63.2$ Å, and also for the same sample that was subsequently partially dried to smaller $D=58.3$ Å. Uncertainties of 10% for K_c and 30% for B were estimated by fitting the data to different regions than the white box in Fig. 1 and by considering different values of the cutoff parameters. The values of K_c in Table I are about 10% larger than the values we previously reported [9]. It is encouraging that K_c is the same for both data sets because K_c should be a material parameter for just a single bilayer. The partially dried sample only requires an osmotic pressure of 1 atm and this is predicted to increase the bilayer thickness by less than 0.1% [6] using data for lateral compressibility K_A [22]. In contrast, even though our estimated uncertainty for B is larger, Table I shows that it increases dramatically as would be expected because the in-

TABLE I. Results for the material parameters of DOPC at $T=30$ °C for two D spacings.

D (Å)	η	ξ	K_c (10^{-13} erg)	B (10^{12} erg/cm^4)
63.2	0.057	52.8	8.0	10.3
58.3	0.027	34.5	8.5	60.1

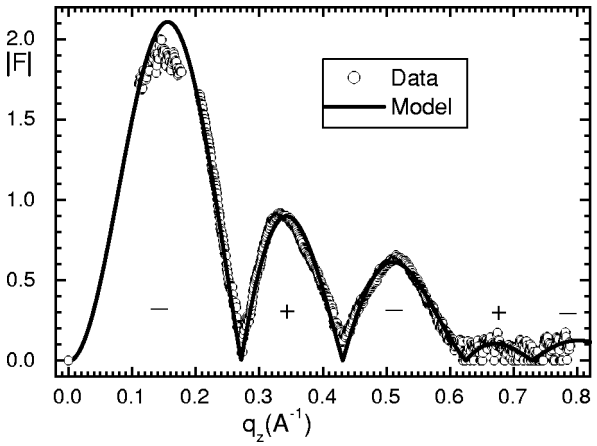

FIG. 3. Results for the bilayer form factor $|F(q_z)|$ (electrons/Å^2) obtained from fitting the off-specular diffuse scattering data with the fluctuation parameters given in Table I.

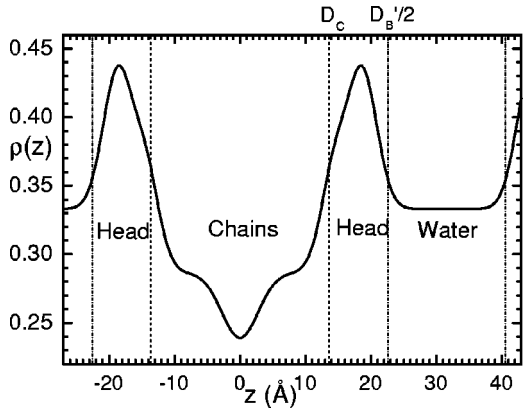

FIG. 4. Electron density profiles $\rho(z)$ (electrons/Å^3) along the z direction perpendicular to DOPC bilayers at 30 °C. The bilayer is symmetric with center at $z=0$; a full water region is shown and the beginning of a second bilayer at $z=40$ Å.

terlamellar interactions are stronger when the water space between bilayers is smaller.

The other factors for the diffuse scattering intensity $I(q)$ are the square of the bilayer form factor $|F(q_z)|^2$ and the Lorentz factor q_z^{-1}. The scaling factors in the fit in Fig. 2 therefore give the form factor shown in Fig. 3. Conventional diffraction methods give $|F(q_h=2\pi h/D)|$ for a few values of h for a considerably smaller range of q_z with hydrated fluid samples, and the ±1 phase factors are not as obvious as they are in Fig. 3. However, for lower q_z the relatively small amount of diffuse scattering compared to the very strong first- and second-order peaks makes $|F(q_z)|$ unreliable in the gap regions in Fig. 3 and the data between the first two peaks is relatively noisy, so a straightforward Fourier inversion to obtain the electron density profile $\rho(z)$ is not directly possible. Fortunately, $F(0)$ is well determined to be very close to zero from volume measurements [19] and the relation [23] $F(0)=2(n_L-V_L\rho_W)/A$, where the electron density of water is $\rho_W=0.333e/\text{Å}^3$ and, per DOPC molecule, $n_L=434$ electrons and $V_L=1303$ Å^3 and the interfacial area $A=72.1$ Å^2 is derived subsequently.

We obtained the electron density profiles shown in Fig. 4 by fitting the data in Fig. 3 to an analytic model [23] that is built from a known constant water electron density ρ_W between bilayers joined by a smooth bridging function in the headgroup region to an unknown constant electron density for the hydrocarbon region. The hydrocarbon region is modified by addition of a negative Gaussian to represent the lower electron density of the terminal methyls on each hydrocarbon chain. Each headgroup is represented by two positive Gaussians, one for the most electron dense phosphate group and a smaller one for the less dense carbonyl groups that connect the hydrocarbon chains to the glycerol backbone. The relative sizes of the headgroup Gaussians were constrained to 1.76 based on simulations [24] and the ratio of terminal methyl volumes to methylene volumes to 1.9 based on simulations [24] and volumetric data [6]. The volume of the headgroup V_H was constrained to $V_H=319$ Å^3 from fully solvated phosphatidylcholine gel phases [6]. Changing these constrained values to other values within their uncertainties or relaxing each of the constraints in turn resulted in little change in the electron density profile shown in Fig. 4 or in the fit to $F(q)$ in Fig. 3 [21]. Simultaneous fits to $|F(q_z)|$ from both samples reported in Table I gave comparable agreement. The fit confirms that the low q_z form factor data near $q_z=0.15$ Å^{-1} are the least reliable. This contrasts with conventional crystallography methodology which is less reliable for higher orders and that therefore gives poorer spatial resolution for smaller regions like the headgroup region.

The most valuable quantity obtained from the electron density profile is the separation D_{HH} of its maxima. This single quantity allows one to bootstrap [25] from the well determined gel phase [1] to determine other valuable quantities [6] such as the interfacial area A, the location D_C of the Gibbs dividing surface for the hydrocarbon region, the number of waters n_W per lipid molecule in the stack, the Luzzati bilayer thickness D_B [26], the steric thickness D_B', and the corresponding thicknesses of the water layers $D_W=D-D_B$ and $D_W'=D-D_B'$. Values of these quantities are given in Table II and D_C and D_B' are shown in Fig. 4.

This method promises to revolutionize the study of membrane structure. The key is that systems with thermodynamic disorder that naturally occurs in the most biologically relevant fully hydrated samples contain much more information in thermal diffuse scattering than in the traditional Bragg peaks. This paper shows that the theory required to extract this information is adequate and that suitable data can be obtained at synchrotrons. A by-product is that the material parameters K_c and B are also obtained. The values of B will be especially important for analyzing the fundamental inter-

TABLE II. Values of structural parameters for DOPC bilayers at 30 °C with units in appropriate powers of angstrom and 1% estimated errors.

A	n_W	D_{HH}	D_C'	D_B	D_B
72.1	32.5	37.1	13.6	45.2	36.1

actions between bilayers [12,26] with the aid of Monte Carlo simulations [27].

We thank many co-workers who have provided essential help over a long time in various aspects of this project. Stephanie Tristram-Nagle prepared the oriented samples using her method [16]. Horia Petrache built the sample chamber under the auspices of Adrian Parsegian. Stephanie Tristram-Nagle, Horia Petrache, John Katsaras, Peter Mason, Georg Pabst, Daniel Harries, Nanjun Chu, and Norbert Kucerka participated in various data collection runs at CHESS (Cornell High Energy Synchrotron Source). We thank Ernie Fontes for getting us started on oriented samples at D1 station at CHESS (NSF Grant No. DMR-9311772) and Ken Finkelstein for helping us to achieve higher resolution at C1 station. This research was supported by the ACS Petroleum Research Fund and by the National Institutes of Health through Grant No. GM44976 (J.F.N.).

[1] S. Tristram-Nagle, Y. Liu, J. Legleiter, and John F. Nagle, Biophys. J. **83**, 3324 (2002).
[2] A. Caillé, C. R. Acad. Sc. Paris: Ser. B. **274**, 891 (1972).
[3] J. Als-Nielsen, J. D. Litster, R. J. Birgeneau, M. Kaplan, C. R. Safinya, A. Lindegaard-Andersen, and S. Mathiesen, Phys. Rev. B **22**, 312 (1980).
[4] J. F. Nagle, R. Zhang, S. Tristram-Nagle, W. Sun, H. Petrache, and R. M. Suter, Biophys. J. **70**, 1419 (1996).
[5] K. Hristova and S. H. White, Biophys. J. **74**, 2419 (1998).
[6] J. F. Nagle and S. Tristram-Nagle, Biochim. Biophys. Acta **1469**, 159 (2000).
[7] R. Zhang, S. Tristram-Nagle, W. Sun, R. L. Headrick, T. C. Irving, R. M. Suter, and J. F. Nagle, Biophys. J. **70**, 349 (1996).
[8] T. Salditt, Curr. Opin. Struct. Biol. **13**, 467 (2003), provides a review, but mistakenly states that the specular and nonspecular scattering are not well separated in the method we use [9].
[9] Y. Lyatskaya, Y. Liu, S. Tristram-Nagle, J. Katsaras, and J. F. Nagle, Phys. Rev. E **63**, 011907 (2001).
[10] F. Nallet, R. Laversanne, and D. Roux, J. Phys. II **3**, 487 (1993).
[11] G. Pabst, M. Rappolt, H. Amenitsch, and P. Laggner, Phys. Rev. E **62**, 4000 (2000).
[12] H. I. Petrache, N. Gouliaev, S. Tristram-Nagle, R. Zhang, R. M. Suter, and J. F. Nagle, Phys. Rev. E **57**, 7014 (1998).
[13] N. Lei, C. R. Safinya, and R. F. Bruinsma, J. Phys. II **5**, 1155 (1995).
[14] T. Salditt, M. Vogel, and W. Fenzl, Phys. Rev. Lett. **90**, 178101 (2003), have mistakenly claimed to have done "the first independent measurement of both elasticity coefficients for a pure phospholipid system without softening additives." Their method takes data at one fixed angle which does not provide the wide q_z range that we analyze.
[15] M. W. Tate, E. F. Eikenberry, S. O. Barna, M. E. Wall, J. L. Lowrance, and S. M. Gruner, J. Appl. Crystallogr. **28**, 196 (1995).
[16] S. Tristram-Nagle, R. Zhang, R. M. Suter, C. R. Worthington, W.-J. Sun, and J. F. Nagle, Biophys. J. **64**, 1097 (1993).
[17] J. Katsaras and M. J. Watson, Rev. Sci. Instrum. **71**, 1737 (2000).
[18] J. Katsaras, Biophys. J. **75**, 2157 (1998).
[19] S. Tristram-Nagle, H. I. Petrache, and J. F. Nagle, Biophys. J. **75**, 917 (1998).
[20] It may be noted that we calculated height-height correlation functions $\langle \mu_0(0)\mu_n(r)\rangle$ for a bulk sample. As shown by R. Holyst, Phys. Rev. A **44**, 3692 (1991); E. A. L. Mol *et al.*, Phys. Rev. E **54**, 536 (1996), the in-plane r dependence should become modified by the solid substrate for lateral distances greater than $R_c = 2\pi\sqrt{t\lambda}$ which is 13 000 Å for our sample thickness $t = 10\ \mu$m and deGennes penetration length $\lambda = 44.1$ Å. Such modifications were not necessary because the long range correlation functions are cut off by L_x and L_y.
[21] Details of the calculations and other aspects of this work may be found in the Ph.D. thesis of Yufeng Liu at http://lipid.phys.cmu.edu/
[22] W. Rawicz, K. C. Olbrich, T. J. McIntosh, D. Needham, and E. A. Evans, Biophys. J. **79**, 328 (2000).
[23] M. C. Wiener, R. M. Suter, and J. F. Nagle, Biophys. J. **53**, 315 (1989).
[24] R. S. Armen, O. D. Uitto, and S. E. Feller, Biophys. J. **75**, 734 (1998).
[25] T. J. McIntosh and S. A. Simon, Biochemistry **25**, 4948 (1986).
[26] R. P. Rand and V. A. Parsegian, Biochim. Biophys. Acta **988**, 351 (1989).
[27] N. Gouliaev and J. F. Nagle, Phys. Rev. Lett. **81**, 2610 (1998).